

A High Efficiency Balanced Frequency Tripler Incorporating Compensation Structure for Millimeter-Wave Applications

Yongjie Liu¹, Minghua Zhao^{1, *}, Zongrui He¹, and Zhongbo Zhu²

Abstract—This paper presents the design and experimental research of a high efficiency balanced frequency tripler in the whole Ka band incorporating compensation solder pads. An anti-parallel GaAs Flip-Chip varistor diode is applied in this frequency tripler. The frequency tripler has the advantages of low conversion loss, broadband and compact circuit size. Considering the parasitic parameters resulted by the actual pads of the nonlinear device, a compensation solder pad was developed and adopted. The conversion loss of the frequency tripler is 15 dB with variation of ± 1 dB across the output frequency from 30 to 37.5 GHz. In experiment, the maximum output power of 5.8 dBm is obtained at 35.4 GHz with 3.8% conversion efficiency when the input power is 20 dBm, and the 3-dB operation band width is about 10 GHz, which shows a good agreement between the simulation results and the experimental results.

1. INTRODUCTION

With the rapid development of millimeter-wave wireless communication in military and commercial applications, such as atmospheric remote sensing, scaled radar range systems, increased security for point-to-point communications, the demand for millimeter-wave source, the key component of the millimeter-wave wireless communication system, is growing. Traditionally, among the methods to obtain the source, the two common ways are fundamental oscillator and frequency multiplier. However, it becomes increasingly difficult to build fundamental frequency oscillators with good power, stability, and noise characteristics when frequency increases into the millimeter-wave range [1]. To overcome this disadvantage, frequency multiplication becomes an efficient way to obtain the millimeter-wave and submillimeter-wave sources [2–4]. From the perspective of the application, a good frequency multiplier should have the characteristics of high output power, low conversion loss and small size. However, design of a good frequency multiplier mostly depends on circuit topology and proper compensation of the parasitic parameters for commercially available discrete Schottky diodes [2]. In order to design a good performance frequency tripler, a simple but effective circuit topology incorporating compensation solder pads is proposed.

Frequency triplers employing an anti-parallel diode pair have been proved to have good performance in millimeter-wave and submillimeter-wave frequency range [5–8]. Compared with the single diode frequency tripler, the frequency triplers based on anti-parallel diodes have major advantages of low spurs and simple idle circuits, because the odd harmonics are combined in phase at the output, while the even harmonics are trapped in the circle of the diode pair. The most important part in the design of a frequency tripler based on anti-parallel diodes is to provide suitable terminations for input frequency and the output frequency at both sides of the diodes [9]. However, the terminations, such as pads,

Received 21 July 2015, Accepted 21 August 2015, Scheduled 9 September 2015

* Corresponding author: Minghua Zhao (minghua3mm@uestc.edu.cn).

¹ EHF Key Lab of Fundamental Science, School of Electronic Engineering, University of Electronic Science and Technology of China, Chengdu 611731, China. ² National Key Laboratory of Space Microwave Technology, China Academy of Space Technology, CAST, Xi'an 710000, China.

of the diodes can also result in parasitic parameters which can affect the performance of the balanced frequency tripler to some extent [10]. Hence, the performance of the balanced frequency tripler can be improved by compensation for the parasitic parameters.

In this work, a balanced frequency tripler incorporating a compensation structure for the parasitic parameter which resulted by the solder pad is proposed. The Schottky diode MA4E1310 is applied as the nonlinear component. In order to predict the performance of the frequency tripler accurately, an accurate equivalent circuit model of the diode is built in the nonlinear simulation platform of advanced design system (ADS). In addition, input and output matching networks are designed and optimized to present proper embedding impedances for the anti-parallel diode pair at corresponding operation frequency, and a microstrip to waveguide transition with low insertion loss is designed and optimized by the simulation platform of high frequency simulation system (HFSS).

2. COMPENSATION SOLDER PAD FOR ANTIPARALLEL DIODE

The solder pad is used to connect the nonlinear device and the linear circuit; however, as operation frequency increases, the parasitic parameters resulted by the pad of the nonlinear device cannot be ignored. In [10], an accurate equivalent circuit of the pad including the relationship between the pad size and the capacitance resulted by the pad of the nonlinear device was proposed. However, for commercially diodes, little work can be done on the pad size. Therefore, to enhance the design reliability and improve the performance of the frequency tripler, a compensation solder pad for antiparallel diode is developed to compensate the capacitance resulted by the pad of the nonlinear device.

In [11], a microstrip structure with insert a narrow transverse slit into a microstrip transmission line, as shown in Figure 1, which can be described in terms of an equivalent series inductivity, is proposed. The value of the equivalent series inductivity is the function of a/W and independent of the slit width b as long as b is roughly between one and one tenth of the substrate thickness. Therefore, the structure can be adopted as the solder pad to compensate the capacitance resulted by the pad of the nonlinear device.

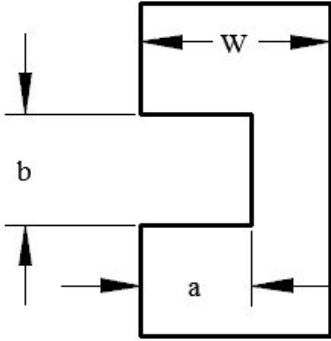


Figure 1. Microstrip transmission line with insert a narrow transverse slit.

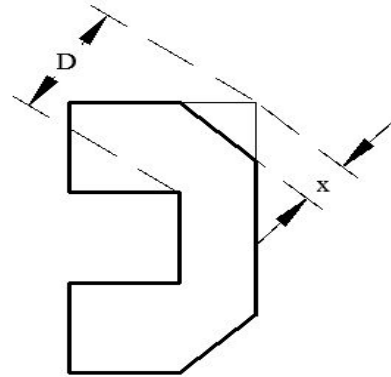


Figure 2. Compensation solder pad.

However, as the solder pad, a disadvantage of the discontinuities at bends still exists, which can cause the degradation in circuit performance. Thus, some changes must be made to eliminate the discontinuities. As shown in Figure 2, the discontinuity at bends is compensated by chamfering which is the traditional and effective method [1]. The variable M is defined as the degree of the chamfering.

$$M = \frac{x}{D} \quad (1)$$

Herein, the compensation solder pad proposed in this work has three advantages.

- 1) The capacitance resulted by the pad of the nonlinear device is compensated by the inductivity provided by the compensation solder pad.

- 2) The discontinuity at bends is compensated by chamfering, which reduce the possibility of mismatch in input and output port.
- 3) The discontinuities between every nonlinear device and the solder pad can be eliminated by tuning the size of the solder pad, which can excite the nonlinear device in a better way.

3. THE CIRCUIT DESIGN OF TRIPLER

3.1. The Circuit Schematic

The proposed frequency tripler in this work is based on anti-parallel diodes. The diagram sketch of the frequency tripler circuit is shown in Figure 3. The input signal is fed into the antiparallel diodes through the optimized input matching network and the left compensation solder pad, while the output circuit is composed of the right compensation solder pad, optimized output matching network and the low insertion loss transition from the microstrip to the waveguide. The input signal excites the anti-parallel diode pair with the same magnitude and 180° out of phase, and the odd harmonics including third harmonic are combined in-phase in the output port, while the even harmonics are trapped in the circle of the diode pair [12].

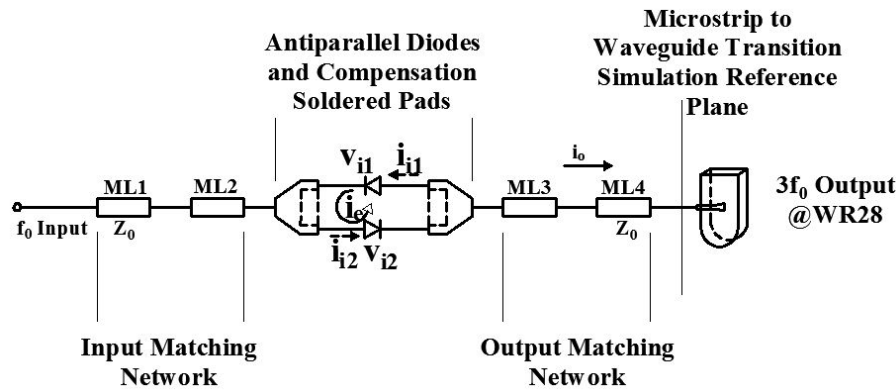


Figure 3. Schematic of the proposed frequency tripler.

The frequency tripler circuit is based on a 0.254-mm thin Rogers5880 substrate (0.254 mm thick, relative dielectric constant 2.22, loss tangent 0.001) and the two M/A-COM MA4E1310 diodes are featured in an antiparallel configuration in this design. The input and output matching network are designed to match to 50 ohm by tuning the widths and electrical lengths of the four microstrip lines ML1, ML2, ML3 and ML4. The compensation solder pads are designed to compensate the capacitance resulted by the pad of the diodes. The third harmonic produced by the anti-parallel diode pair is coupled to the output, and the *E*-plane probe transition from microstrip to standard WR28 waveguide is designed to reduce the propagation loss and cut off the fundamental frequency.

Generally, to obtain accurate simulation results, frequency tripler circuits are simulated and optimized by the combination of nonlinear and linear simulation platforms with ADS and HFSS. The linear circuit is divided into three sub-circuit blocks that are simulated separately by the HFSS to obtain the precise *S*-parameters of the three sub-circuit blocks, which presents the characterization of the linear circuit. The *S*-parameters corresponding to different blocks are combined with the equivalent circuit model of the nonlinear device built in ADS to simulate and optimize in terms of conversion efficiency and output power.

3.2. Theory Analysis

The proposed frequency tripler utilizes the principles of traditional balanced frequency multiplier. As shown in Figure 3, the upper and lower diodes are connected with the compensation solder pads on

both sides of the diode pair. The results of the frequency tripler are that the odd harmonics flow to the output port, which can be well explained by the following equations.

The currents' flow direction of the diodes marked at Figure 3 is applied to help explain the flow direction of the even harmonics and odd harmonics. As analysis in the previous, V_{i1} and V_{i2} are of the same in magnitude ($V_{i1} = V_{i2} = V_i$) and 180° out of phase. The currents I_{i1} and I_{i2} are excited by the voltages V_{i1} and V_{i2} , respectively, and because of the nonlinear characteristic of the diodes, the currents I_{i1} and I_{i2} can be expressed as:

$$I_{i1} = I_s \cdot (\exp(r \cdot V_{i1}) - 1) \tag{2}$$

$$I_{i2} = I_s \cdot (\exp(-r \cdot V_{i2}) - 1) \tag{3}$$

where r is a constant which determined by the diode and I_s the reverse saturate current of the diode.

Thus, the signal coupled to the output port can be expressed as:

$$I_o = I_{i1} - I_{i2} = 2I_s \cdot \sinh(r \cdot V_i) \tag{4}$$

The signal trapped in the circuit of the diode pair can be expressed as:

$$I_e = I_{i1} + I_{i2} = 2I_s \cdot \cosh(r \cdot V_i) - 2I_s \tag{5}$$

Apparently, according to (2), (3), (4) and (5), the currents flowing toward to the output port are all odd harmonics, while the all even harmonics and DC currents are trapped in the circuit of the diode pair.

3.3. Diode Equivalent Circuit

The nonlinear diodes are the essential and most important part in the design of a frequency multiplier, which greatly affects the performance of the design [6, 9, 12]. In order to get a multiplier with better

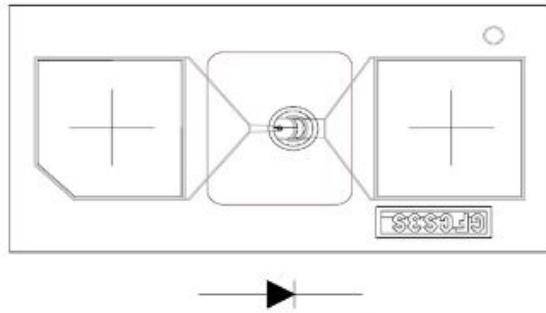


Figure 4. The overview of the diode.

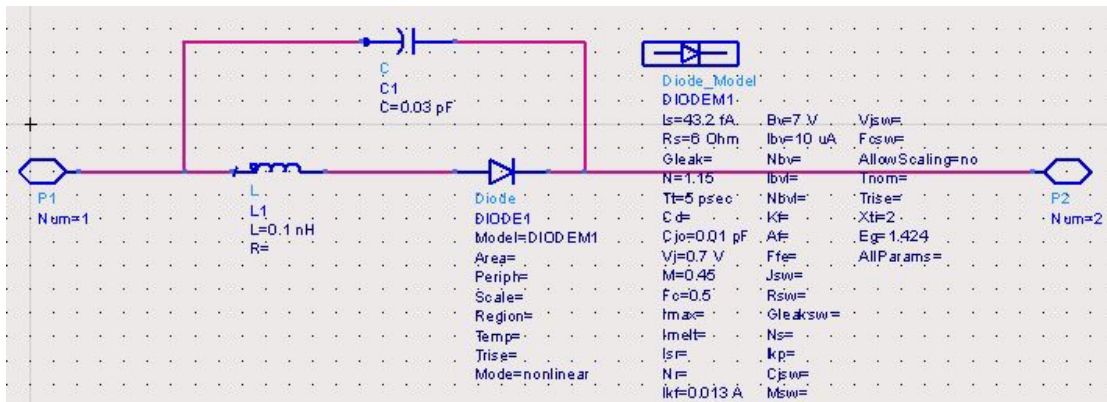


Figure 5. MA4E1310 diode equivalent circuit.

performance, much attention must be paid to the diode selection and the establishment of diode equivalent circuit.

Among the existing diodes, Schottky diodes have been widely used in multipliers and mixers and proved to have good performance because of its high switching speed which was suitable for high frequency range [13, 14]. In this work, commercially available GaAs Schottky barrier diode MA4E1310 from M/A-COM company was adopted as the nonlinear device, and Figure 4 shows the overview of the diode. The main characteristics of this diode are allowing use through millimeter wave frequencies, high breakdown voltage: $< -4.5\text{ V}@10\ \mu\text{A}$, and extremely low parasitic.

In Ka-band, the analytical nonlinear diode model provided by the fast harmonic-balance simulator ADS can describe the nonlinear characteristics of the diode. In addition, the parasitic parameters provided by its datasheet can be equivalent to corresponding lumped elements [9, 13]. In [9], an effective way to establish the diode equivalent circuit was introduced. Furthermore, the SPICE parameters of the diode can be extracted by the I-V curve and C-V curve [15]. The main nonlinear spice parameters of MA4E1310 diode extracted by the I-V curve are summarized in Table 1. Figure 5 shows the equivalent circuit for the diode in ADS. Figure 6 shows the comparison between the simulation I-V curve and the I-V curve provided by the datasheet at room temperature. From Figure 6, the result shows a good agreement between the I-V curve provided by the datasheet of the diode and the I-V curve simulated by the ADS.

Table 1. Main nonlinear SPICE parameters of MA4E1310 Schottky diode.

R_s (ohm)	I_s (fA)	C_{j0} (pF)	N	I_{bv} (μA)
6	43.2	0.01	1.15	10

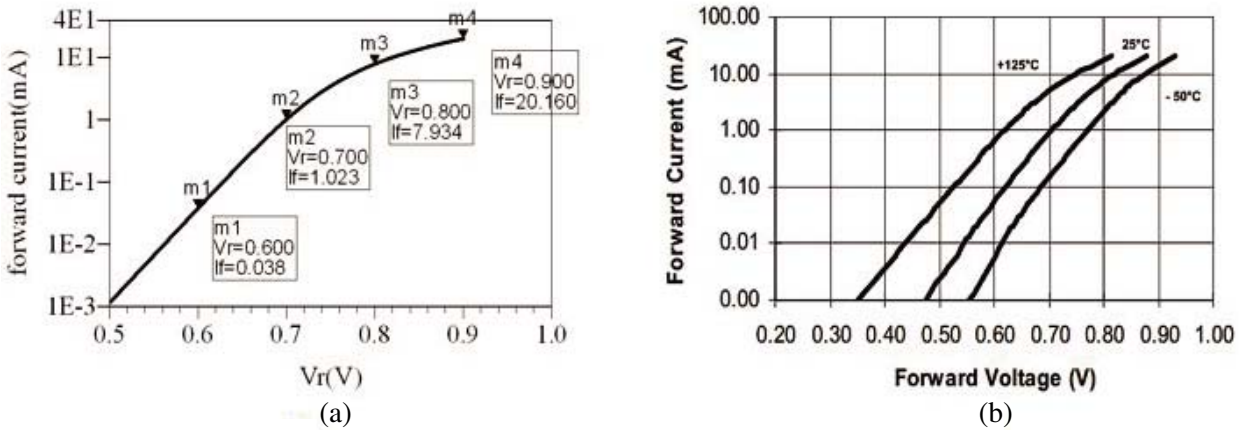


Figure 6. (a) I-V curve obtained through ADS simulation, (b) typical I-V curve provided by the varistor diode data sheet.

3.4. Microstrip to Waveguide Transition

As the non-negligible loss produced by the transition from microstrip to coaxial line in welding when frequency increases into the millimeter wave range, the transition from microstrip to waveguide is adopted as an essential part in millimeter-wave circuits design because of its simple structure and low insertion loss [16, 17]. In this work, a low insertion loss transition from microstrip to the standard WR-28 rectangular waveguide via an E -plane probe is proposed.

Figure 7 shows the sketch of the proposed transition. The transition consists of WR28 rectangular waveguide, E -plane probe (P_ML3), high-impedance line (P_ML2) and 50 ohm microstrip line (P_ML1). The input signal is coupled to the output port by the E -plane probe, and the high-impedance line is

used to compensate for the capacitive reactance produced by the *E*-plane probe [16]. Therefore, the performance of the transition is greatly affected by both the *E*-plane probe and the high-impedance line. Thus, better performance of the transition can be achieved by tuning the P_ML2, P_ML3 and D marked at Figure 7.

The transition is simulated and optimized by the simulator ofHFSS. The simulation results of the transition are presented in Figure 8, and the corresponding electrical lengths of the P_ML1, P_ML2 and P_ML3 are shown in Table 2.

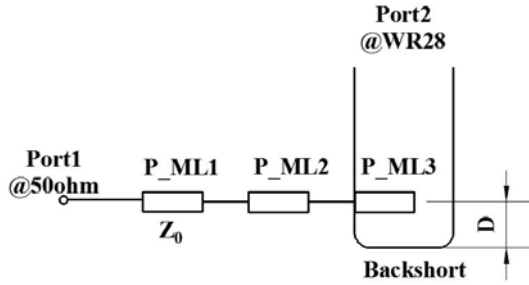


Figure 7. Sketch of the transition.

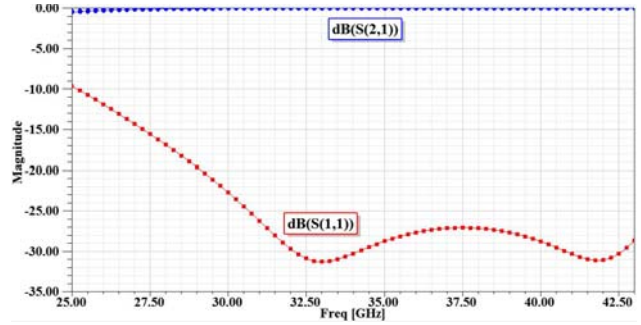


Figure 8. Simulated *S*-parameters of the transition.

Table 2. Structure size of the symbols (UNIT: mm).

Symbol	P_ML1	P_ML2	P_ML3	<i>D</i>
Length (mm)	3.23	0.77	1.72	2.05
Width (mm)	0.72	0.54	1.03	

3.5. Simulations of the Frequency Tripler

As introduced above, the HFSS is employed to build the 3-D electromagnetic model of the whole frequency tripler and simulate the linear response of the frequency tripler. Figure 9 shows the overall model built in HFSS. The compensated pads with labels Port #1~#4 are also shown.

The ADS is applied to simulate the nonlinear response of the frequency tripler with combining the 6-port *S*-parameters file exported from the 3-D EM model of the frequency tripler shown in Figure 9.

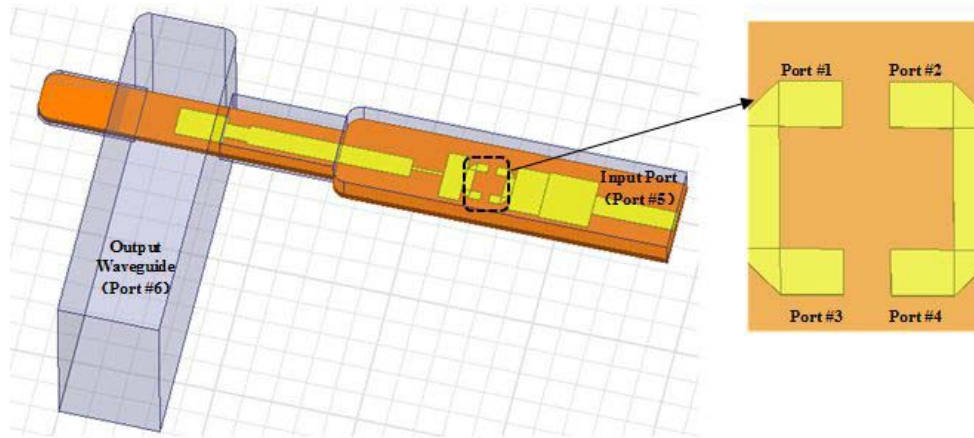


Figure 9. 3-D electromagnetic circuit model of the frequency tripler.

The 6-port S -parameters file well presents the port match state and the transmission loss resulted by the guide waveguide and the microstrip line, which contributes to predict the performance of the frequency tripler accurately. Combing with the diode model mentioned above, the schematic drawing of the integrated model built in ADS is shown in Figure 10.

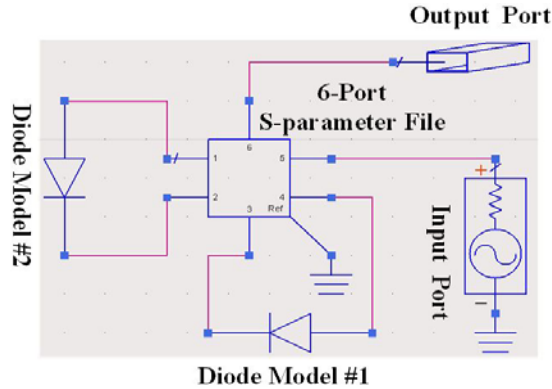


Figure 10. Integrated model for nonlinear simulation.

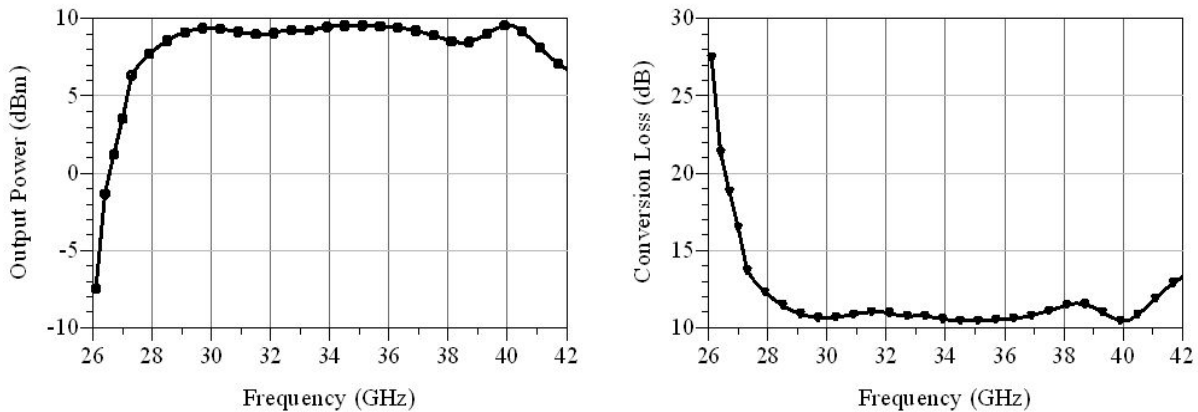


Figure 11. Simulated output power and conversion loss of the frequency tripler when pumped with 20 dBm of input power.

The overall simulation is performed with 20 dBm input power. Figure 11 shows the simulated output power and the conversion. In the whole Ka-band, the output power is above 5 dBm, and the maximum output is 9.8 dBm with 10.2 dB conversion loss at 40 GHz. In addition, the output power is 9 dBm with variation of ± 1 dB across 28 GHz to 40 GHz. Because of the frequency selection of the microstrip to waveguide transition, the output power declines quickly from 5 dBm to -7.5 dBm with frequency lower than 26.5 GHz.

It can be concluded from Figure 8 and Figure 11 that the operation bandwidth of the frequency tripler has great relationship with the transition from microstrip to waveguide, and the compensation solder pads can contribute to the improvement of the performance of the frequency tripler.

4. EXPERIMENTS OF THE FREQUENCY TRIPLER

The circuit of the frequency tripler is fabricated on an RT/Rogers 5880 substrate with thickness of 0.254 mm and relative dielectric constant of 2.22. Figure 12 shows the circuit layout of the frequency tripler, and the measurement system is composed of an Agilent signal generator E8267D, transition



Figure 12. The circuit layout of the frequency tripler.

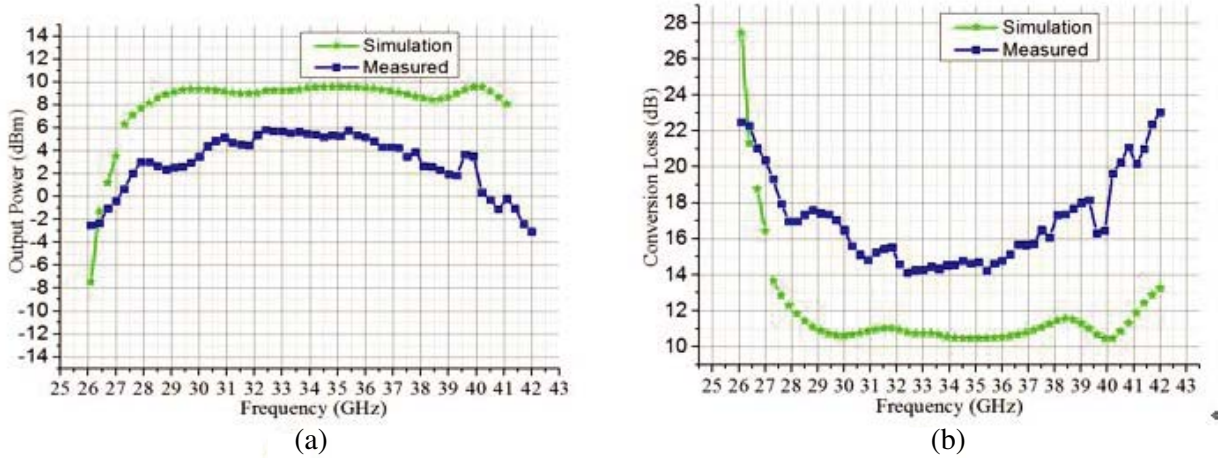


Figure 13. (a) The measured and simulated output power, (b) the measured and simulated conversion loss.



Figure 14. The photograph of the frequency tripler.

from WR28 waveguide to coaxial line and an Agilent frequency analyzer N9030A. The upper frequency limits of the E8267D and N9030A in laboratory are 43.5 GHz and 44 GHz, respectively, which can well satisfy the demand of the test.

In experiment, the frequency tripler exhibits output power above 0 dBm from 27 GHz to 40 GHz, and the maximum output power is 5.8 dBm with 3.8% frequency multiplication efficiency at input frequency of 11.8 GHz with input power of 20 dBm. The conversion loss of the frequency tripler is about 15 dB with variation of ± 1 dB across the 30–38 GHz band. The 3-dB band width is from 30 GHz to 40 GHz. The measured output power and efficiency of the frequency tripler are shown in Figure 13. The assembled frequency tripler block is shown in Figure 14, and the whole size of the tripler is 40 mm \times 20 mm \times 20 mm.

Compared with the simulation curve in Figure 11, the measured results are well consistent with the simulation results in the whole Ka-band.

5. CONCLUSIONS

In this work, a high efficiency balance passive frequency tripler with compensation solder pad has been designed, fabricated, and measured. This frequency tripler consists of a microstrip embedding circuit with compensation solder pads, a pair of M/A-COM GaAs Schottky barrier diode featured in an antiparallel configuration and waveguide-to-microstrip transition. A compensation structure solder is adopted to improve the performance of the frequency tripler obviously, and an accurate design method of the combination of electromagnetic simulation and nonlinear character simulation is adopted to predict the performance of the tripler.

The test data for the 35.4 GHz show 5.8 dBm output power with 3.8% efficiency. The 3-dB band width is 10 GHz. The measured results agree well with the simulation ones, which demonstrates that the balance frequency tripler with compensation solder pad has good performance and can be applied in Ka-band communication and radar system.

ACKNOWLEDGMENT

This work is supported by the EHF Key Laboratory of Fundamental Science Fund of No. A03011023801006001 and No. A03010023801171002, and is also supported by the Laboratory Fund of No. 9140A21010214HT05 and No. 9140C530404130C53193.

REFERENCES

1. Pozar, D. M., *Microwave Engineering*, 3rd Edition, 599–608, 2005.
2. Chen, Z. and J. Xu, “Design and characterization of a W-band power-combined frequency tripler for high-power and broadband operation,” *Progress In Electromagnetics Research*, Vol. 134, No. 1, 133–150, 2013.
3. Erickson, N. R., et al., “High efficiency MMIC frequency triplers for millimeter and submillimeter wavelengths,” *IEEE MTT-S International Microwave Symposium Digest, IEEE MTT-S International Microwave Symposium*, Vol. 2, 1003–1006, 2000.
4. Zhao, M., Y. Fan, D. Wu, and J. Zhan, “The investigation of W band microstrip integrated high order frequency multiplier based on the nonlinear model of Avalanche diode,” *Progress In Electromagnetics Research*, Vol. 85, 439–453, 2008.
5. Guo, J., J. Xu, and C. Qian, “A new scheme for the design of balanced frequency tripler with Schottky diodes,” *Progress In Electromagnetics Research*, Vol. 137, No. 9, 407–424, 2013.
6. Chen, Z. and J. Xu, “Design of a W-band frequency tripler for broadband operation based on a modified equivalent circuit model of GaAs Schottky varistor diode,” *Journal of Infrared Millimeter & Terahertz Waves*, Vol. 34, No. 1, 28–41, 2013.
7. Morgan, M. and S. Weinreb, “A full waveguide band MMIC tripler for 75–110 GHz,” *IEEE MTT-S International Microwave Symposium Digest, IEEE MTT-S International Microwave Symposium*, Vol. 1, 103–106, 2001.
8. Porterfield, D. W., et al., “A high-power fixed-tuned millimeter-wave balanced frequency doubler,” *IEEE Transactions on Microwave Theory & Techniques*, Vol. 47, No. 4, 419–425, 1999.
9. Zeljami, K., J. Gutierrez, J. P. Pascual, T. Fernandez, A. Tazon, and M. Boussouis, “Characterization and modeling of Schottky diodes up to 110 GHz for use in both flip-chip and wire-bonded assembled environments,” *Progress In Electromagnetics Research*, Vol. 131, No. 5, 457–475, 2012.
10. Li, X. and J. Gao, “Pad modeling by using artificial neural network,” *Progress In Electromagnetics Research*, Vol. 74, 167–180, 2007.
11. Hofer, W. J. R., “Equivalent series inductivity of a narrow transverse slit in microstrip,” *IEEE Transactions on Microwave Theory & Techniques*, Vol. 25, No. 10, 822–824, 1977.
12. Guo, J., J. Xu, and C. Qian, “Design of dual-mode frequency multiplier with Schottky diodes,” *IEEE Microwave & Wireless Components Letters*, Vol. 24, No. 8, 554–556, 2014.

13. Liew, Y. H. and J. Joe, "Large-signal diode modeling — An alternative parameter-extraction technique," *IEEE Transactions on Microwave Theory & Techniques*, Vol. 53, No. 8, 2633–2638, 2005.
14. Xue, Q., K. M. Shum, and C. H. Chan, "Low conversion-loss fourth subharmonic mixers incorporating CMRC for millimeter-wave applications," *IEEE Transactions on Microwave Theory & Techniques*, Vol. 51, No. 5, 1449–1454, 2003.
15. Mass, S. A., "Nonlinear microwave and RF circuits," *Microwave Journal*, May 2003.
16. Aliakbarian, H., A. Enayati, G. A. E. Vandebosch, and W. De Raedt, "Novel low-cost end-wall microstrip-to-waveguide splitter transition," *Progress In Electromagnetics Research*, Vol. 101, 75–96, 2010.
17. Tang, W. and X. B. Yang, "Design of Ka-band probe transitions," *2011 International Conference on IEEE Applied Superconductivity and Electromagnetic Devices (ASEMD)*, 2011.